

UC San Diego

UC San Diego Previously Published Works

Title

Multivariable Feedback Relevant System Identification of a Wafer Stepper System

Permalink

<https://escholarship.org/uc/item/4w58n954>

Journal

IEEE Transactions on Control Systems Technology, 9(2)

Author

De Callafon, Raymond

Publication Date

2001-03-01

Peer reviewed

Multivariable Feedback Relevant System Identification of a Wafer Stepper System

Raymond A. de Callafon and Paul M. J. Van den Hof

Abstract—This paper discusses the approximate and feedback relevant parametric identification of a positioning mechanism present in a wafer stepper. The positioning mechanism in a wafer stepper is used in chip manufacturing processes for accurate positioning of the silicon wafer on which the chips are to be produced. The accurate positioning requires a robust and high-performance feedback controller that enables a fast throughput of silicon wafers. A control relevant set of multivariable finite dimensional linear time invariant discrete-time models is formulated and estimated on the basis of closed-loop experiments. The set of models is shown to be suitable for model-based robust control design of the positioning mechanism; this is illustrated by a successful design and implementation of a robust controller.

Index Terms—Closed-loop identification, motion control systems, positioning systems, robust control, system approximation, system identification.

I. INTRODUCTION

WAFER steppers combine a high accuracy positioning and a sophisticated lithographic process to manufacture integrated circuits (chips) via a fully automated process. By means of a photolithographic process, the chip architecture is exposed on the surface of a wafer, a silicon disk covered with photo resist. In the application discussed in this paper, the wafer is supposed to carry approximately 80 chips. In order to expose the surface of the wafer, each chip is processed sequentially. Such a sequential process is needed as only one mask of the chip layout is available during the exposure phase of the photolithographic process. For that purpose, the wafer is placed on a moving table that needs to be accurately moved (stepped) in three degrees of freedom (3DOF) for the sequential processing of the chips on the wafer.

Clearly, both the accuracy and the speed of the servo mechanism during the subsequent steps of the wafer will influence the

success and throughput of the production process of the chips on the wafer. Sophisticated control of this (multivariable) servo mechanism can help in achieving a required throughput by designing a multivariable feedback controller that is able to satisfy high performance requirements [8]. A model that describes the dynamical behavior of the servo mechanism is needed to design such a controller thoughtfully.

A dynamical model can be obtained by first principle modeling, see, e.g., [8]. Although such a model provides valuable knowledge of the dynamical behavior, either the numerical completion of specific elements in the servo system is undiscoverable or deliberate assumptions are posed to simplify the modeling. This causes the model to deviate from the actual dynamical behavior of the system. Alternatively, a system identification procedure can be exploited in which experimental data is used directly. In this way, a model describing the dynamical behavior is evaluated directly on the basis of the data coming from the actual system [13].

Although both modeling procedures provide insight in the dynamical behavior of the positioning mechanism present in a wafer stepper, it is impossible to exactly characterize all phenomena describing the dynamics. On the one hand, exact modeling can be impossible or too costly. On the other hand, control design methods can get unmanageable if they are applied to models of high complexity. As a result, the model obtained is only an approximation of the system to be controlled. As the validity of any approximate model hinges on its intended use, the modeling procedure being applied should take into account the intended use of the model (control design).

II. MODELING FOR CONTROL

In this paper the attention is focused on deriving finite-dimensional linear time invariant (FDLTI) models via system identification techniques that approximates the dynamical behavior of the positioning mechanism in a wafer stepper. For an existing servo mechanism present in a wafer stepper, time domain observations are gathered to estimate models that can be used for subsequent controller design. The aim of this paper is to outline the system identification procedure being used and the performance improvement obtained when designing a multivariable controller.

In order to estimate models suitable for control design, the following requirements should be satisfied. Preferably, the models should be a linear description of the actual system to be controlled. In this way, standard tools for linear model-based

Manuscript received November 25, 1999; revised June 6, 2000. Recommended by Associate Editor F. Doyle. This work was supported by Philips Research Laboratories, Eindhoven, the Netherlands. The work of R. A. de Callafon was supported by the Dutch Graduate School on Systems and Control. This work is part of the research program of the "Stichting voor Fundamenteel Onderzoek der Materie" (FOM), which is financially supported by the Nederlandse Organisatie voor Wetenschappelijk Onderzoek (NWO).

R. A. de Callafon was with the Mechanical Engineering Systems and Control Group, Delft University of Technology, 2628 CJ Delft, The Netherlands. He is with the Department of Mechanical and Aerospace Engineering, University of California, San Diego, La Jolla, CA 92093-0411 USA (e-mail: callafon@ucsd.edu).

P. M. J. Van den Hof was with the Mechanical Engineering Systems and Control Group, Delft University of Technology. He is now with the Department of Applied Physics, Delft University of Technology, 2628 CJ Delft, The Netherlands (e-mail: p.m.j.vandenhof@tn.tudelft.nl).

Publisher Item Identifier S 1063-6536(01)01805-X.

control design can be used.¹ Furthermore, control design methods become unmanageable if they are applied to models of high complexity. Hence, linear models should have a reasonable model order in order to formulate a manageable control design problem. As the models will be necessarily approximative, it should contain those dynamical aspects that are important for control design [20]. Finally, the identification procedure being used should be able to deal with data that is obtained under closed-loop (controlled) conditions. This is due to the fact that many engineering systems are unable to operate without additional control, including the position servo mechanism of the wafer stepper.

Estimating a linear model can be done by existing system identification techniques reported in the literature [13], [22] and available in the corresponding commercial software packages [14]. However, application of these techniques to find models on the basis of closed-loop experiments that capture the dominant dynamical aspects relevant for feedback, is far from trivial. Estimating such models boils down to the fact that models, suitable for control design, can only be found by taking the closed-loop operation of the model into account [19]. In general, this leads to an identification problem in which the criterion used for designing the subsequent controller should also be used to deduct the model. See, for example, the work by [27] for LQG-based controller design, and [23] for an overview of approaches.

As the resulting model is just an approximation of the system to be identified, the controller based on the model has to be robust against any dissimilarities between the model and the system. This has been a motivation for the development of identification techniques that estimate an upper bound on the model error, see, for example, the contributions by [10], [12], [15], [18], and the references therein. The resulting model error constitutes an allowable model perturbation around a nominal model being estimated and defines a set of models where the actual system is assumed to be an element of. Subsequently, a robust controller can be designed on the basis of this set of models [9]. In this approach stability and performance requirements are guaranteed for the complete set of models, that includes the actual system to be controlled. The estimation of such a set of models for the design of a robust controller for the positioning mechanism of the wafer stepper is the main item in this paper.

In order to estimate such a set of models by the estimation of a (low complexity) nominal model along with its allowable model perturbation, the identification procedure discussed in this paper uses the algebraic framework of stable fractional model representations, similarly as in [6] or [24]. The reasoning to use such a fractional model representations is due to the ability to deal with both stable, unstable or marginally unstable systems, such as the positioning mechanism discussed in this paper. As such, this approach enables one to find a set of feedback relevant models by estimating stable factorizations of a nominal model along with a stable perturbation on the allowable model perturbations. Furthermore, the fractional approach can deal with observations obtained under closed-loop (con-

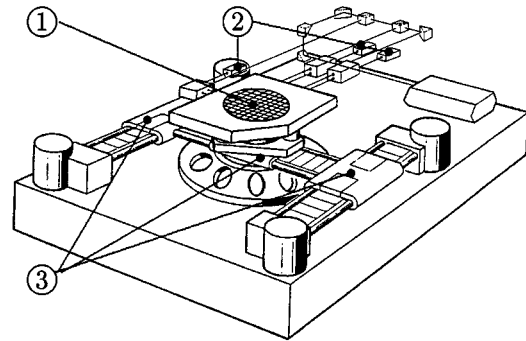


Fig. 1. Schematic view of wafer stage; 1: Wafer chuck, 2: Laser interferometers, 3: Linear motors.

trolled) conditions relatively easily. The theoretical background for the approach presented in this paper is more extensively discussed in [5] and [7].

III. WAFER STEPPER SERVO MECHANISM

A. Description of Servo Mechanism

The servo mechanism discussed in this paper is an integral part of the Silicon Repeater 3rd generation (SIRE3) wafer stepper. The moving table, called the wafer chuck, that needs to position the wafer, is equipped with an air bearing and placed on a large suspended granite block to reduce the effect of external vibrations. The position of the wafer chuck on the horizontal surface of the granite block is measured by means of laser interferometry. A schematic overview of this servo mechanism is depicted in Fig. 1.

Relative movements of the wafer chuck are measured by determining the phase shift of the laser beams reflected on the mirror block depicted in Fig. 1. As the horizontal plane allows three degrees of freedom, three laser measurements uniquely determine the horizontal position of the wafer, whereas three linear motors are used to position the wafer chuck in 3DOF. This makes the servo mechanism of the wafer stepper a multivariable system, having three inputs and three outputs. The inputs reflect the currents to the three linear motors, whereas the outputs are constructed by measuring the position of the wafer chuck both in x -, y -direction (translation), and the ϕ -direction (rotation).

B. Experimental Setup

In order to perform an identification and to test the control of the servo mechanism, an experimental set up has been provided by the Philips Research Laboratories and has been depicted in Fig. 2.

The experimental set up is equipped with a computer interface to measure the position in x -, y -, and ϕ -direction of the wafer chuck on discrete time samples via a digital signal processor. Due to safety requirements and operating conditions of the laser interferometers, the signals can be measured only if a (digital) controller is used to control the positioning of the wafer chuck. Such a digital controller can be implemented using the same digital signal processor.

Consequently, only (discrete-time) measurements obtained under feedback can be gathered for identification purposes. Additional external reference signals can be applied to the feed-

¹Although linear models are used, it can be noted here that the modeling and design tools proposed in this paper will include nonlinear and iterative optimization techniques to find optimal models and controllers with a linear structure.

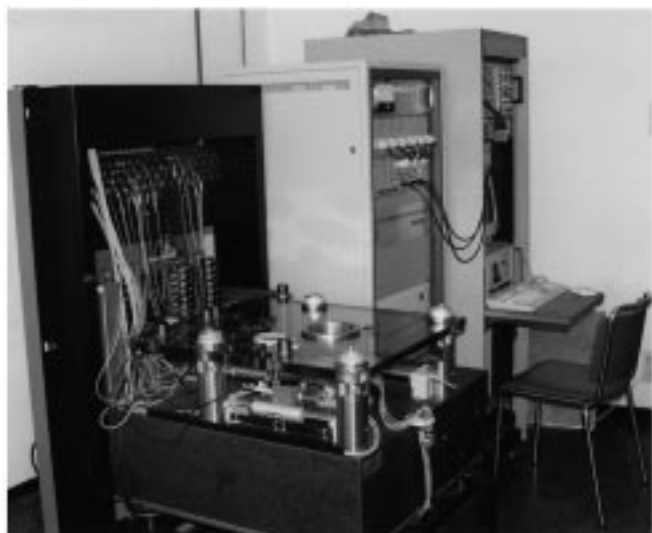


Fig. 2. Photo of experimental setup.

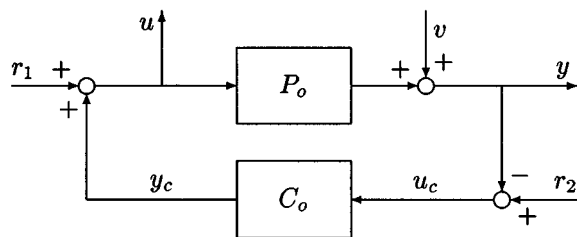


Fig. 3. Block diagram of experimental setup of feedback controlled positioning mechanism.

back connection of the positioning mechanism to provide sufficient excitation [13] while gathering data for identification. A schematic overview of the signals that can be accessed in the feedback connection is depicted in the block diagram of Fig. 3.

As indicated in Fig. 3, the positioning mechanism of the wafer chuck is denoted by P_o , while the feedback controller currently used to control P_o is denoted by C_o . In the current experimental set up, the controller C_o consists of three parallel PID controllers controlling the positioning in x -, y -, and ϕ -direction separately. The feedback connection of P_o and the controller C_o is denoted by $T(P_o, C_o)$.

C. Control of the Positioning Mechanism

Next to the purpose of providing sufficient excitation of $T(P_o, C_o)$, the reference signals in Fig. 3 can be used to move or step the wafer chuck in a desired direction. As such, the signals r_1 and r_2 can be used to evaluate the performance of the feedback controlled positioning mechanism by applying a reference signal r_2 and a feedforward signal r_1 in order to track a certain desired position signal y of the wafer chuck. In this way, the input signal u_c to the controller C_o reflects the servo error between a desired reference r_2 and the actual desired position y .

Controlling the positioning mechanism of the wafer chuck aims at minimizing the servo error, while moving the chuck as fast as possible. The design specification for the SIRE3 wafer stepper is to bring the servo error within a bound of 52 nm (four

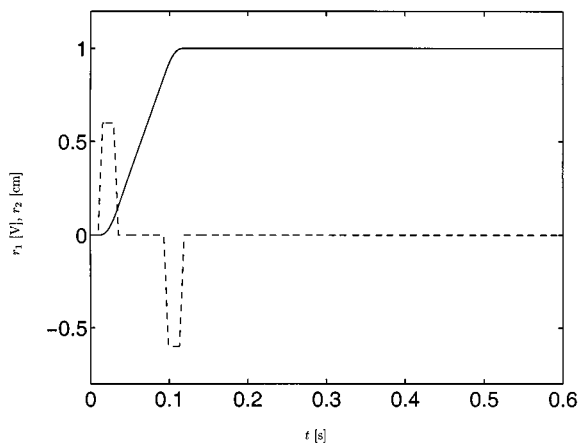


Fig. 4. Shape of reference signal r_2 (—) and feedforward signal r_1 (- -).

times the measurement resolution) as soon as possible after a step has been performed. This is due to the fact that the chuck must be kept in a constant position before a chip can be exposed on the surface of the wafer.

Henceforth, controlling the positioning of the wafer chuck requires the combined design of both a feedback controller and the appropriate reference r_2 and feedforward signal r_1 [8]. In this paper, however, the attention is focused on the identification of a set of models, denoted by \mathcal{P} , to improve the design of the feedback controller only.

In order to compare feedback controllers designed on the basis of the set of models \mathcal{P} being estimated, the signals r_2 and r_1 are fixed to some prespecified desired trajectory. This prespecified trajectory is based on the dominating open-loop dynamical behavior of P_o that is given by a double integrator, relating the force generated by the linear motors to the position of the wafer chuck. Based on this relatively simple model, r_2 will denote a desired position profile, whereas r_1 denotes (a scaled) acceleration profile obtained by computing the second derivative of r_2 . A typical shape of the reference signal r_2 and the feedforward signal r_1 to position the wafer chuck in either the x - or y -direction over 1 cm is depicted in Fig. 4.

In Fig. 4, the position profile r_2 is obtained by allowing a maximum jerk (derivative of acceleration) and a maximum speed of the wafer chuck. The resulting acceleration profile r_1 is the second derivative of r_2 . Although optimal reference signals can be designed for finite time optimal control problems, step wise reference signals are being used here only to compare the positioning performance due to feedback. Application of both reference signals in either an x - or y -direction is labeled as a step, respectively, in x - or y -direction. Using these specified reference signals r_1 and r_2 for the current experimental setup in which three parallel PID controllers are used to control the positioning in x -, y -, and ϕ -direction separately, the servo error $u_{c,x}$ depicted in Fig. 5 for a step in the x -direction is obtained.

It can be observed from Fig. 5 that the servo error $u_{c,x}$ is hardly within the bounds of 52 nm indicated by the dotted lines. Furthermore, $u_{c,x}$ exhibits a low frequent vibration after the step has ended. As a result, the settling time of the step is strongly influenced and both an improvement of the speed of decay and a reduction of the low-frequency vibration of

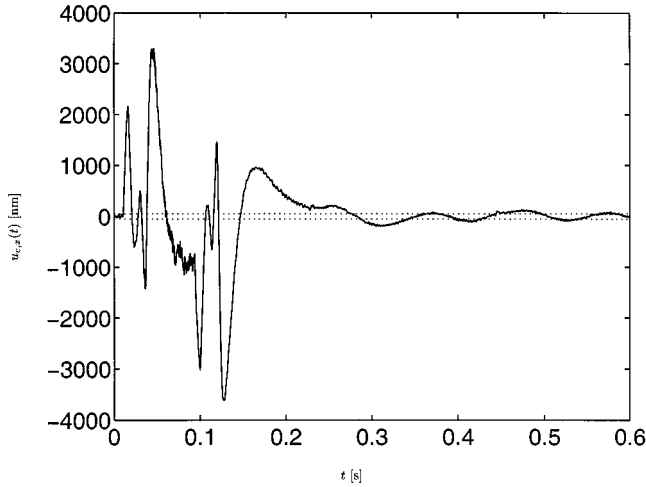


Fig. 5. Servo error response to a step in x -direction.

the servo error is desired to improve the behavior of the servo mechanism. Clearly, the process under consideration exhibits dynamic phenomena additional to the simple model of a double integrator. Characterization of these dynamics in a way relevant for control design is essential in achieving maximum performance of the positioning mechanism in the wafer stepper.

IV. PRELIMINARIES

A. Data Obtained from Experimental Setup

For analysis purposes, P_o is considered to be a discrete-time linear time invariant map that is characterized by the difference equation

$$y(t) = P_o(q)u(t) + v(t)$$

where

- t = $k\Delta T$;
- $k = 0, 1, 2, \dots$ discrete-time character of the signals being processed by the digital processor;
- $qu(t) = u(t+1)$ forward shift;
- u and y input (currents to the linear motors) and a disturbed output (measured position in x -, y -, and ϕ -direction), respectively, of the positioning mechanism.

The signal v is used to model the disturbance that may be present on the output y . The signals u and y are measurable and sampled with a sampling time $\Delta T = 0.3$ ms, while known reference signals r_1 and r_2 are applied to provide sufficient excitation of $T(P_o, C_o)$.

It is assumed that the feedback connection $T(P_o, C_o)$ is well posed, that is $\det(I + C_o P_o) \neq 0$ [1] and the mapping from the signals $\text{col}(r_2, r_1)$ onto $\text{col}(y, u)$ is given by the transfer function matrix $T(P_o, C_o)$ with

$$T(P_o, C_o) := \begin{bmatrix} P_o \\ I \end{bmatrix} (I + C_o P_o)^{-1} [C_o \quad I] \quad (1)$$

where $\text{col}(\cdot)$ refers to the operation of stacking two vectors in one column. As a result, the data obtained from the feedback connection $T(P_o, C_o)$ of Fig. 3 can be described by

$$\begin{bmatrix} y \\ u \end{bmatrix} = T(P_o, C_o) \begin{bmatrix} r_2 \\ r_1 \end{bmatrix} + \begin{bmatrix} I \\ -C_o \end{bmatrix} (I + P_o C_o)^{-1} v. \quad (2)$$

For identification purposes, it is presumed that the noise v is uncorrelated with the external reference signals r_1, r_2 and that it can be modeled as the output of a monic stable and stably invertible noise filter H_0 having a white noise input e [13].

B. Norm-Based Control Design

In order to design the feedback controller, a norm-based control design will be used. In this way, the design specifications are translated in a control objective function, whereas a norm of the function is used to indicate the performance of the resulting feedback connection. For notational convenience a control objective function is denoted by a stable rational function $J(P, C)$, where P and C are FDLTI (possibly unstable) mappings and used to denote, respectively, a system and a feedback controller. The notion of performance will be characterized by the value of the norm $\|J(P, C)\|_\infty$: a smaller value of $\|J(P, C)\|_\infty$ indicates better performance [23].

The mapping from the reference signals (r_2, r_1) to the output and input signals (y, u) of the plant P_o is given by the matrix $T(P_o, C_o)$ in (1). In a similar way, a feedback connection of a system P and a controller C can be studied by inspecting the matrix $T(P, C)$ with

$$T(P, C) := \begin{bmatrix} P \\ I \end{bmatrix} (I + CP)^{-1} [C \quad I]. \quad (3)$$

Note that a feedback connection $T(P, C)$ is internally stable if and only if $T(P, C)$ is stable [21]. In order to incorporate control design specification for the map $T(P, C)$, the control objective function $J(P, C)$ is taken to be a weighted form of the matrix $T(P, C)$ given in (3) and is defined as follows:

$$\|J(P, C)\|_\infty := \|U_2 T(P, C) U_1\|_\infty \quad (4)$$

where U_2 and U_1 are (square) weighting functions. The weighting functions U_1 and U_2 are chosen in such a way that the bandwidth of the resulting feedback connection can be adjusted, which will increase the speed of decay of the resulting servo error depicted in Fig. 5. Furthermore, the weighting functions can be used to design a controller C that allows for an additional suppression of the low-frequency vibration of the servo error.

In this particular situation the weighting functions are chosen to comply with a loop shaped situation; by choosing

$$U_2 = \begin{bmatrix} U_l & 0 \\ 0 & U_r^{-1} \end{bmatrix} \quad U_1 = U_2^{-1}$$

the performance objective function J can be written as

$$J(G, C) = \begin{bmatrix} U_l G \\ U_r^{-1} I \end{bmatrix} [I + CG]^{-1} [C U_l^{-1} \quad U_r] \quad (5)$$

$$= T(G_{ls}, C_{ls}) \quad (6)$$

with

$$G_{ls} = U_l G U_r \quad (7)$$

$$C = U_r C_{ls} U_l. \quad (8)$$

The performance characterization (4) is fairly general and will be used for analysis purposes in this paper. In this perspective, the performance objective function $J(P, C)$ as given in (4) will be used to evaluate both the identification of a set of models \mathcal{P} and the additional reduction of a robust controller designed based on the set \mathcal{P} . For that purpose, the set of models \mathcal{P} as used in this paper is discussed below.

C. Characterization of the Set of Models

In order to design a robust controller for the positioning mechanism of the wafer stepper, the estimation of a single approximate (nominal) model does not suffice. To be robust against any dissimilarities between a model and the actual system P_o , a set of models \mathcal{P} needs to be estimated. Such a set of models allows one to capture the actual system P_o in the robust controller design, provided that $P_o \in \mathcal{P}$. An (upper) LFT

$$\mathcal{F}_u(Q, \Delta) := Q_{22} + Q_{21}\Delta(I - Q_{11}\Delta)^{-1}Q_{12} \quad (9)$$

provides a general notation to represent all models $P \in \mathcal{P}$ as follows:

$$\mathcal{P} = \{P | P = \mathcal{F}_u(Q, \Delta) \text{ with } \Delta \in R\mathcal{H}_\infty \text{ and } \|\Delta\|_\infty < 1\}$$

where Δ indicates an unknown (but bounded) uncertainty. The entries of the coefficient matrix Q in (9) dictate the way in which the set of models \mathcal{P} is being structured. As a special entry one can recognize the nominal model, denoted by \hat{P} , for which $\Delta = 0$

$$\hat{P} := \mathcal{F}(Q, 0) = Q_{22}.$$

Employing the knowledge of the controller C_o implemented on the system P_o for experimental considerations, the set of models \mathcal{P} will be characterized by using the algebraic theory of fractional model representations [25]. In this way, the coefficient matrix Q in (9) is formed by considering a model perturbation that is structured according to a Youla-Kucera parameterization. Following this parameterization, the set of models used in this paper is structured as follows:

$$\mathcal{P} = \{P | P = (\hat{N} + D_c \bar{\Delta})(\hat{D} - N_c \bar{\Delta})^{-1} \\ \text{with } \bar{\Delta} \in R\mathcal{H}_\infty \text{ and } \|\hat{V} \bar{\Delta} \hat{W}\|_\infty < 1\} \quad (10)$$

where (N_c, D_c) and (\hat{N}, \hat{D}) , respectively, denote a right coprime factorization (*rcf*) of the controller C_o implemented on the system P_o and a nominal model \hat{P} , that satisfies $T(\hat{P}, C_o) \in R\mathcal{H}_\infty$. The (stable and stably invertible) weighting functions \hat{V} , \hat{W} are used to normalize the upper bound on $\hat{V} \bar{\Delta} \hat{W}$.

Particular advantages of this uncertainty structure are that, by construction, all models in \mathcal{P} are guaranteed to be stabilized by C_o ; additionally the evaluation of the performance cost function $J(P, C_o)$ becomes relatively simple due to the fact that it turns

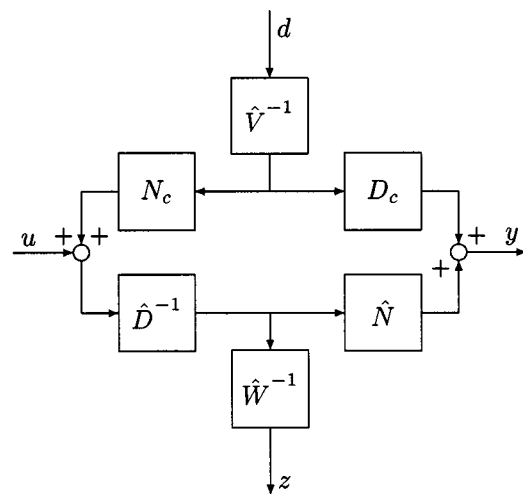


Fig. 6. Block diagram of LFT representation.

out to be affine in $\bar{\Delta}$. This latter mechanism will be further explained in Section VI.

The LFT characterization of the models P within the set of models of (9) can be represented by the block diagram given in Fig. 6. It can be verified from the map $col(d, u)$ to $col(z, y)$ in Fig. 6 that the coefficient matrix Q in the LFT of (9) is given by

$$Q = \left[\begin{array}{c|c} \hat{W}^{-1} \hat{D}^{-1} N_c \hat{V}^{-1} & \hat{W}^{-1} \hat{D}^{-1} \\ \hline (D_c + \hat{P} N_c) \hat{V}^{-1} & \hat{P} \end{array} \right]. \quad (11)$$

Consequently, the matrix Q contains all the relevant information in order to characterize the set of models \mathcal{P} . In (11), the nominal model \hat{P} , or its *rcf* (\hat{N}, \hat{D}) , and the stable and stably weighting filters \hat{V} and \hat{W} are the unknown quantities to be estimated.

D. Feedback Relevant Identification

To control the complexity of the controller being designed, it is required to bound the complexity of the nominal model (\hat{N}, \hat{D}) and the weighting filters (\hat{V}, \hat{W}) . By again exploiting the knowledge of the controller C_o , an approximate identification of both a nominal model and the weighting filters can be tuned toward the intended control application. In other words, a set of models \mathcal{P} , subjected to the condition $P_o \in \mathcal{P}$, should be estimated such that

$$\sup_{P \in \mathcal{P}} \|J(P, C_o)\|_\infty \quad (12)$$

is minimized. In this way, a set of models is found for which the worst case performance for the controller C_o is minimized.

Minimizing (12) using the limited complexity *rcf* (\hat{N}, \hat{D}) and weighting filters (\hat{V}, \hat{W}) simultaneously is intractable. Therefore, minimization of (12) is tackled by estimating the *rcf* (\hat{N}, \hat{D}) and the pair (\hat{V}, \hat{W}) separately. Clearly, by the separate identification of the *rcf* (\hat{N}, \hat{D}) of a nominal model \hat{P} and the weighting filters (\hat{V}, \hat{W}) only an upper bound on (12) can be minimized. However, available tools for the identification of a nominal factorization and an uncertainty bound can be exploited to complete the estimation of the set of models.

V. ESTIMATION OF A NOMINAL MODEL

A. Access to Coprime Factorizations

The first step in the characterization of the set of models \mathcal{P} , is the (approximate) identification of a stable nominal factorization (\hat{N}, \hat{D}) of a (possibly unstable) nominal model \hat{P} . Access to a *rcf* of the system P_o for identification purposes can be obtained by a simple filtering of the signals present in the feedback connection $\mathcal{T}(P_o, C_o)$.

Inspecting (2), the transfer functions $(P_o S_{\text{in}}, S_{\text{in}})$, with $S_{\text{in}} = (I + C_o P_o)^{-1}$, can be considered to be a stable (right) factorization of the system P_o with $P_o = [P_o S_{\text{in}}][S_{\text{in}}]^{-1}$. Denoting $r := r_1 + C_o r_2 = u + C_o y$ it can be observed that $(P_o S_{\text{in}}, S_{\text{in}})$ is accessible from data as u and y are measured. To avoid the presence and estimation of common unstable zeros in the stable right factorization of P_o , the factorization needs to be a *rcf*. Furthermore, a *rcf* is not unique and access to different factorizations would be preferable.

As indicated in [24] or [4], an additional filtering of the reference signal r via $x := Fr$ is possible. With (2) this yields

$$x = F \begin{bmatrix} C_o & I \end{bmatrix} \begin{bmatrix} r_2 \\ r_1 \end{bmatrix} = F \begin{bmatrix} C_o & I \end{bmatrix} \begin{bmatrix} y \\ u \end{bmatrix} \quad (13)$$

and (2) reduces to

$$\begin{bmatrix} y \\ u \end{bmatrix} = \begin{bmatrix} P_o S_{\text{in}} F^{-1} \\ S_{\text{in}} F^{-1} \end{bmatrix} x + \begin{bmatrix} (I + P_o C_o)^{-1} \\ -C_o (I + P_o C_o)^{-1} \end{bmatrix} v \quad (14)$$

where $(P_o S_{\text{in}} F^{-1}, S_{\text{in}} F^{-1})$ can be considered to be a (right) factorization of the system P_o . In order for this factorization to be *right coprime* the filter F in (13) is restricted to the form

$$F = [D_x + C_o N_x]^{-1} \quad (15)$$

where (N_x, D_x) is a *rcf* of any auxiliary model P_x that is stabilized by C_o . For more details on this characterization, see [24]. This includes choices for F that achieve normalization of the factorization $(N_{o,F}, D_{o,F})$ which has the additional advantage that redundant dynamics in the two factors is removed.

Consequently, a simple filtering (13) of the signals present in the feedback connection $\mathcal{T}(P_o, C_o)$ allows the access to a *rcf* of the system P_o . The system equation (2) can then be written in the form

$$\begin{bmatrix} y \\ u \end{bmatrix} = \begin{bmatrix} N_{o,F} \\ D_{o,F} \end{bmatrix} x + \begin{bmatrix} I \\ -C_o \end{bmatrix} [I + P_o C_o]^{-1} v \quad (16)$$

where x is given in (13), F is given in (15) and $(N_{o,F}, D_{o,F})$ is the *rcf* of the plant P_o given by

$$\begin{bmatrix} N_{o,F} \\ D_{o,F} \end{bmatrix} = \begin{bmatrix} P_o \\ I \end{bmatrix} [I + C P_o]^{-1} [I + C P_x] D_x. \quad (17)$$

Since x in (13) is uncorrelated with v , (16) gives rise to an equivalent open-loop identification problem of the *rcf* $(N_{o,F}, D_{o,F})$ of the system P_o .

B. Feedback Relevant Estimation of Coprime Factorizations

In the estimation of the *rcf* (\hat{N}, \hat{D}) , minimization of (12) must be taken into account when estimating a nominal factorization (\hat{N}, \hat{D}) . Furthermore, $\hat{P} = \hat{N}\hat{D}^{-1}$ is subjected to in-

ternal stability of the feedback connection $\mathcal{T}(\hat{P}, C_o)$ in order to characterize the set of models \mathcal{P} given in (10).

Clearly, at this stage the set of models \mathcal{P} is unknown and (12) cannot be computed. In fact, the set of models \mathcal{P} is arbitrarily large as the norm bounded uncertainty $\bar{\Delta}$ in (10) has not been characterized. Consequently, for any nominal model \hat{P} there exists a norm bounded uncertainty $\bar{\Delta}$ that forms a set of models \mathcal{P} for which $P_o \in \mathcal{P}$. As $P_o \in \mathcal{P}$, for any nominal model $\hat{P} \in \mathcal{P}$ the following upper bound for $\|J(\hat{P}, C_o)\|_\infty$ can be given:

$$\begin{aligned} \|J(\hat{P}, C_o)\|_\infty \\ \leq \|J(P_o, C_o)\|_\infty + \|J(\hat{P}, C_o) - J(P_o, C_o)\|_\infty. \end{aligned}$$

As $\|J(P_o, C_o)\|_\infty$ in the above expression does not depend on the nominal model \hat{P} , the upper bound can be minimized by an estimated *rcf* (\hat{N}, \hat{D}) of a nominal model that minimizes

$$\|J(\hat{P}, C_o) - J(P_o, C_o)\|_\infty \quad (18)$$

thus constituting a control-relevant identification criterion.

With the expressions introduced above, it can be shown [4] that

$$\begin{aligned} J(P_o, C_o) - J(\hat{P}, C_o) \\ = U_2 \left(\begin{bmatrix} N_{o,F} \\ D_{o,F} \end{bmatrix} - \begin{bmatrix} \hat{N} \\ \hat{D} \end{bmatrix} \right) F \begin{bmatrix} C_o & I \end{bmatrix} U_1 \quad (19) \end{aligned}$$

where (\hat{N}, \hat{D}) satisfies the constraint $\hat{D} + C_o \hat{N} = F^{-1}$.

The estimation of a nominal factorization for the positioning mechanism of the wafer stepper will be illustrated in the next section.

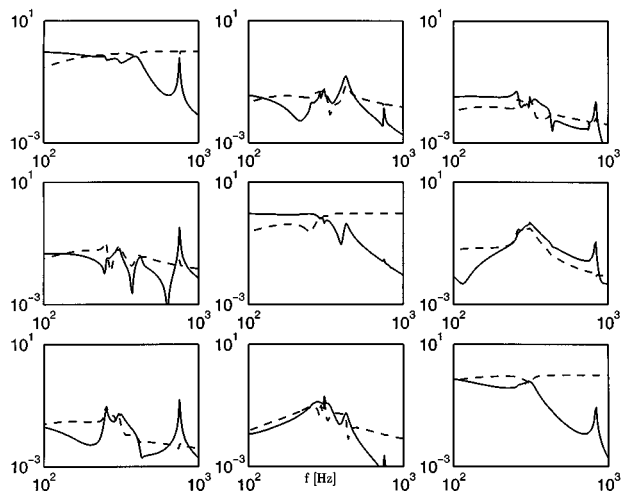
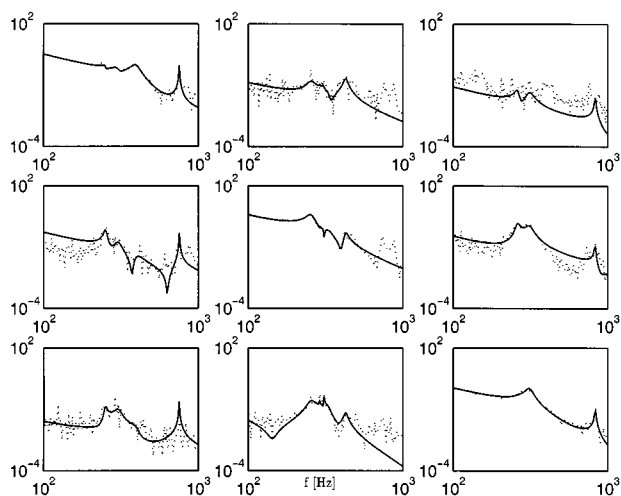
C. Estimation of Nominal Factorizations

To estimate a nominal factorization (\hat{N}, \hat{D}) , frequency domain measurements of the factorization $N_{o,F}(\omega), D_{o,F}(\omega)$ along a prespecified frequency grid are used. The external signals r_1 and r_2 are both excited with (uncorrelated) periodic signals, being random phased sequences of 200 sinusoids. For identification purposes, 50 periods of 2048 data points are taken into account.

Subsequently, the curve fitting procedure described in [3] is used to tackle the weighted minimization of (18) and (19) frequency wise. As the curve fitting procedure is a nonlinear optimization, an initial estimate is required to start the optimization. For that purpose, a multivariable least squares curve fitting procedure is used [2].

An amplitude Bode plot of the *rcf* (\hat{N}, \hat{D}) being estimated can be found in Fig. 7. The resulting estimate of $\text{col}(\hat{N}, \hat{D})$ is a 30th-order discrete-time multivariable model having six inputs and three outputs. Computing $\hat{P} = \hat{N}\hat{D}^{-1}$ yields a 30th-order nominal model, having three inputs and three outputs. The amplitude bode plot of the model \hat{P} , along with the available frequency domain data computed via $N_{o,F}(\omega)D_{o,F}(\omega)^{-1}$ is depicted in Fig. 8.

In this estimation problem an 18th-order curve-fitted plant model is used to design the weighting functions U_1 and U_2 . They are designed to achieve decoupling of the multivariable plant at 90 Hz, and a nominal bandwidth of approximately 90 Hz.


 Fig. 7. Amplitude bode plot of estimated coprime factors \hat{N} (—) and \hat{D} (- -).

 Fig. 8. Amplitude bode plot of computed \hat{P} (—) and frequency domain data (\cdots).

Furthermore, two integrators are incorporated in each diagonal transfer of the loop-shaped plant.

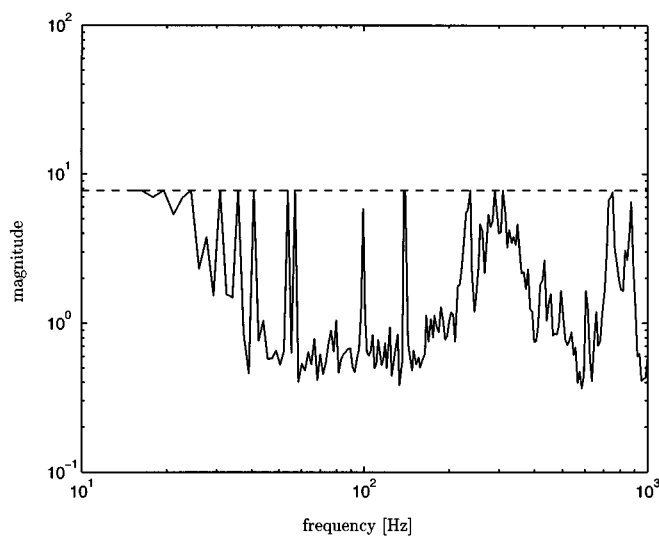
Although stability of $T(\hat{P}, C_o)$ is not guaranteed by the estimation of the coprime factorization (\hat{N}, \hat{D}) discussed here, the model \hat{P} is stabilized by C_o . This is mainly due to the fact that a good fit of the frequency domain data is obtained in the closed-loop relevant frequency area around 200 Hz.

The result of the \mathcal{H}_∞ -norm minimization (18) is visualized in Fig. 9, where the maximum singular value $\bar{\sigma}$ of $J(P_o, C_o) - J(\hat{P}, C_o)$ is sketched. Note that $\|\cdot\|_\infty := \max_\omega \bar{\sigma}$.

VI. ESTIMATION OF MODEL UNCERTAINTY BOUNDS

A. Access to Model Uncertainty

Once a *rcf* of a nominal model is obtained, an estimation of the allowable model perturbation $\bar{\Delta}$ in (10) can be performed. This involves the characterization of an upper bound on $\bar{\Delta}$ in (10) via the stable and stably invertible filters (\hat{V}, \hat{W}) such that (12) is being minimized and $P_o \in \mathcal{P}$. For that purpose, first (an upper bound on) the allowable model perturbation $\bar{\Delta}$ is de-


 Fig. 9. Evaluation of $\bar{\sigma}[J(P_o, C_o) - J(\hat{P}, C_o)]$ over the frequency grid.

termined by applying a model error bounding estimation technique. The uncertainty estimation routine described by [11] is used to obtain a frequency dependent upper bound for $\bar{\Delta}$

$$\|\bar{\Delta}(\omega)\| \leq \delta(\omega) \text{ with probability } \geq \alpha \quad (20)$$

where α is a prechosen probability. In the multivariable case, the upper bound (20) can be obtained for each transfer function. Subsequently, stable and stably invertible weightings \hat{V} and \hat{W} can be determined that overbound the estimated upper bound $\delta(\omega)$.

Clearly, in order to estimate a frequency dependent upper bound on $\bar{\Delta}$, the map $\bar{\Delta}$ must be accessible from data. This can be achieved by defining the signal

$$z := (D_c + \hat{P}N_c)^{-1} [I \quad -\hat{P}] \begin{bmatrix} y \\ u \end{bmatrix} \quad (21)$$

which can be shown to satisfy

$$z = \bar{\Delta}x + D_c(I + P_o C_o)^{-1}v. \quad (22)$$

As x is uncorrelated with v this points to an open-loop bounded error identification problem to find an upper bound for a stable $\bar{\Delta}$. The estimated upper bound of $\bar{\Delta}$ in (20) can then be used to complete the characterization of the set of models \mathcal{P} .

B. Feedback Relevant Estimation of Model Uncertainty

Limiting the complexity of a controller designed on the basis of the set of models \mathcal{P} being identified also requires the complexity of the weighting filters (\hat{V}, \hat{W}) in (11) to be bounded. As a consequence, the estimated upper bound $\delta(\omega)$ in (20) needs to be approximated and over bounded by low-complexity weighting filters (\hat{V}, \hat{W}) . Using the LFT representation of the set of models \mathcal{P} given in (11), the performance of any (newly designed) controller C applied to any model $P \in \mathcal{P}$ can be rewritten in terms of an LFT (5)

$$J(P, C) = \mathcal{F}_u(M, \Delta) \quad \forall P \in \mathcal{P}$$

where the entries of M are given by

$$\begin{aligned} M_{11} &= -\hat{W}^{-1}(\hat{D} + C\hat{N})^{-1}(C - C_o)D_c\hat{V}^{-1} \\ M_{12} &= \hat{W}^{-1}(\hat{D} + C\hat{N})^{-1}[C \ I]U_1 \\ M_{21} &= -U_2 \begin{bmatrix} -I \\ C \end{bmatrix} (I + \hat{P}C)^{-1}(I + \hat{P}C_o)D_c\hat{V}^{-1} \\ M_{22} &= U_2 \begin{bmatrix} \hat{N} \\ \hat{D} \end{bmatrix} (\hat{D} + C\hat{N})^{-1}[C \ I]U_1. \end{aligned} \quad (23)$$

It can be observed from (23) that substitution of $C = C_o$ yields $M_{11} = 0$. This implies that when the controller C_o is applied to the estimated set of models \mathcal{P} , the upper LFT $\mathcal{F}_u(M, \Delta)$ modifies into

$$M_{22} + M_{21}\Delta M_{12} \quad (24)$$

which is an affine expression in Δ . Substituting M_{21} and M_{12} in (24) with $\Delta = \hat{V}\bar{\Delta}\hat{W}$ yields the following expression:

$$M_{22} + M_{21}\Delta M_{12} = M_{22} + W_2\bar{\Delta}W_1$$

where

$$\begin{aligned} W_2 &= -U_2 \begin{bmatrix} -D_c \\ N_c \end{bmatrix} D_c \\ W_1 &= \hat{D}^{-1}(I + C_o\hat{P})^{-1}[C_o \ I]U_1. \end{aligned} \quad (25)$$

Consequently, the effect of replacing an accurate (and high-order estimate) of the upper bound $\bar{\Delta}$ by a low-order upper bound approximation $\tilde{\Delta}$ on the (robust) performance $\|J(P_o, C_o)\| = \|M_{22} + W_2\bar{\Delta}W_1\|$ can be bounded by the following triangular inequality:

$$\|M_{22} + W_2\bar{\Delta}W_1\| \leq \|M_{22} + W_2\tilde{\Delta}W_1\| + \|W_2(\bar{\Delta} - \tilde{\Delta})W_1\|. \quad (26)$$

From (26) it can be observed that, similar to identification of a low-complexity factorization of a nominal model, a weighted difference between the actual and highly complex uncertainty $\bar{\Delta}$ and the low complexity approximation $\tilde{\Delta}$ must be taken into account. The weightings W_2 and W_1 are given in (25) and are known, once a nominal factorization (\hat{N}, \hat{D}) has been estimated.

C. Estimation of Model Uncertainty

Given the nominal factorization (\hat{N}, \hat{D}) and a normalized *rcf* (N_c, D_c) of the controller C_o , an estimation of the allowable model perturbation $\bar{\Delta}$ in (10) is performed. For that purpose, the uncertainty estimation as presented in [11] has been applied to estimate a frequency dependent upper bound on $\bar{\Delta}$. A complete discussion on the uncertainty estimation procedure of [11] is beyond the scope of this paper. Here we will just point to its main characteristics

- It combines a worst-case bounding of unmodeled dynamics with a probabilistic bound on the variance error;
- It employs linearly parameterized models (basis functions) for which least-squares or IV estimates are constructed;

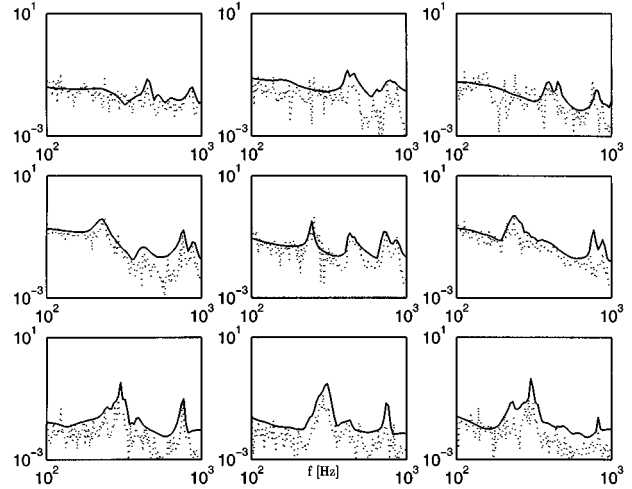


Fig. 10. Amplitude bode plot of estimated uncertainty bound $\delta(\omega)$ (—) of $\bar{\Delta}$ and frequency domain estimate of Δ (···).

- Uncertainty regions for frequencies in any user-chosen frequency grid are computed from bias and variance errors.

The result of this procedure is presented in Fig. 10.

It can be observed from Fig. 10 that the upper bound of the frequency domain estimation of $\bar{\Delta}$ is crossing the upper bound $\delta(\omega)$. Partly, this is due to the fact the upper bound only holds within a prespecified probability of 95%.

VII. USING THE IDENTIFIED SET FOR CONTROL DESIGN

On the basis of the identified set of models, a robust controller was designed via a μ -synthesis [28]. As $\delta(\omega)$ is only a frequency dependent upper bound for $\bar{\Delta}$, low frequent weighting filters (\hat{V}, \hat{W}) are used to parameterize the upper bound on the estimated uncertainty bound $\delta(\omega)$ depicted in Fig. 10. In this way, the estimated upper bound can be taken into account during a robust controller design.

In the construction of (\hat{V}, \hat{W}) the weightings W_1 and W_2 given in (25) are used to emphasize the frequency range for the upper bounding of $\delta(\omega)$ by the parametric stable and stably invertible weightings (\hat{V}, \hat{W}) . It can be observed from (25) that the input sensitivity $(I + C_o\hat{P})^{-1}$, based on the nominal model \hat{P} , is incorporated in the weightings given in (25). As a consequence, the weightings emphasize (again) the closed-loop relevant frequency area around 200 Hz.

Extracting the controller C from the LFT given in (23), a lower LFT $\mathcal{F}_l(G, C)$ can be obtained for the synthesis of a robust controller. In this lower LFT the map G is given by

$$\begin{bmatrix} \hat{W}^{-1} & 0 & 0 \\ 0 & U_2 & 0 \\ 0 & 0 & I \end{bmatrix} \begin{bmatrix} \hat{D}^{-1}N_c & 0 & \hat{D}^{-1} & \hat{D}^{-1} \\ (D_c + \hat{P}N_c) & 0 & \hat{P} & \hat{P}_i \\ 0 & 0 & I & I \\ -(D_c + \hat{P}N_c) & I & -\hat{P} & -\hat{P} \end{bmatrix} \cdot \begin{bmatrix} -\hat{V}^{-1} & 0 & 0 \\ 0 & U_1 & 0 \\ 0 & 0 & I \end{bmatrix}.$$

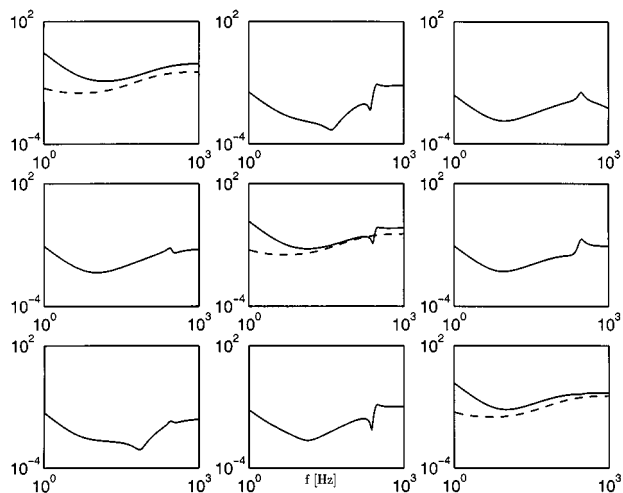


Fig. 11. Amplitude Bode plot of old controller C_o (dashed) and newly designed controller C (solid).

Invoking the μ -design, a high-order multivariable feedback controller is obtained. In order to implement the controller being designed, an additional closed-loop controller reduction [26] was used to reduce the controller to a 32nd-order state-space realization. A comparison between the controller C_o previously implemented on the system P_o and the newly designed controller C is given in terms of the amplitude Bode plot depicted in Fig. 11.

Compared to the initial controller it can be seen that the newly designed C is a multivariable controller. Furthermore it has additional dynamics to account for the modeled (uncertain) mechanical resonance modes of the plant P_o . Before implementing the new controller the robust performance and stability need to be evaluated. This can be carried out with the estimated set of models \mathcal{P} . This is done by evaluating $\|J(P, C)\|_\infty$ for all models $P \in \mathcal{P}$.

To evaluate the performance (robustness) of the newly designed controller C , in Fig. 12 the structured singular value $\mu\{M(e^{i\omega})\}$ has been plotted point wise over the frequency domain range between 10 and 1000 Hz, for both the present controller C_o and the newly designed controller C . It can be seen that the new controller C has improved the performance by lowering the maximum of the structured singular value $\mu\{M(e^{i\omega})\}$ with a factor of approximately four.

As a result, the performance index $\|J(P, C)\|_\infty$ evaluated for all models $P \in \mathcal{P}$ with the new controller C is guaranteed to be approximately four times better and as a result the performance of the closed-loop system has been improved.

For presentation purposes, the weighting functions \hat{V} and \hat{W} in (10) are scaled to normalize the uncertainty $\bar{\Delta}$. As a result, performance robustness for the performance criterion (4) is guaranteed if $\max_\omega \mu\{M(e^{i\omega})\} < 1$. It can be seen from Fig. 12 that this is not that case, but by adjusting the performance weighting functions U_1 and U_2 used in the performance characterization (4), performance robustness can be enforced for a specific (nominal) performance criterion $\|U_2 T(P, C) U_1\|_\infty$.

Whether or not the performance weighting functions U_1 and U_2 are adjusted to guarantee performance robustness, the performance of the newly designed controller C can be shown to be

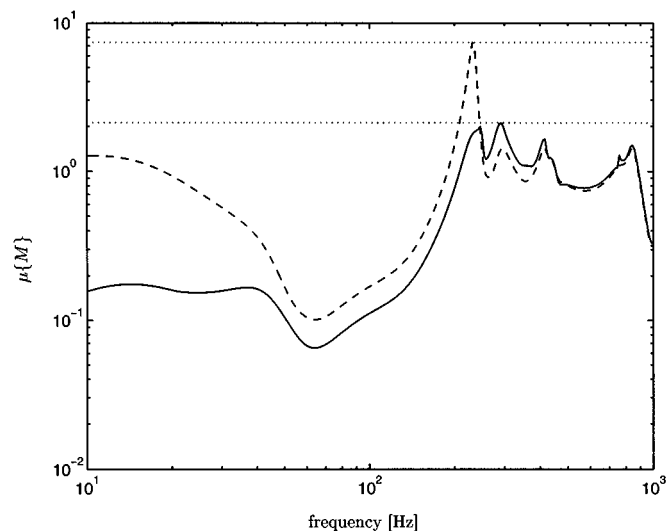


Fig. 12. Structured singular value $\mu\{M(e^{i\omega})\}$ for present controller C_o (dashed) and new controller C (solid).

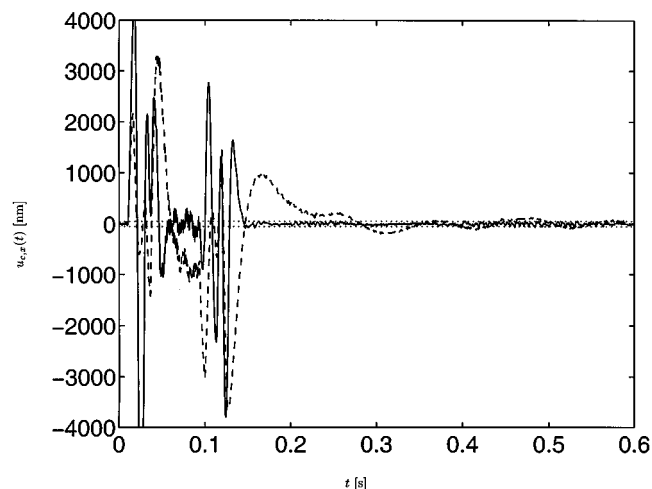


Fig. 13. Servo error response to a step in x -direction with old controller C_o (dashed) and new controller C (solid).

improved over the present controller C_o . Moreover, irrespective of the performance weighting functions U_1 and U_2 , stability robustness is guaranteed due to the coprime factor nature of the set of models \mathcal{P} . As a result, the newly designed controller C can be implemented and has a guaranteed improved performance compared to the present controller C_o .

In order to illustrate the improved performance of the positioning control, the reference signals r_1 and r_2 depicted in Fig. 4 are put on the newly designed feedback connection $T(P_o, C)$. A comparison with the servo error of Fig. 5 obtained with the previous controller C_o is depicted in Fig. 13. It can be seen from Fig. 13 that both the speed and the accuracy of positioning have been improved successfully.

VIII. CONCLUSION

This paper discusses the approximate and feedback relevant parametric identification of a servo mechanism present in a wafer stepper. Via the identification of a set of models, built up from a nominal model along with an allowable model

perturbation, the dynamical behavior of the servo mechanism has been modeled.

The feedback relevant identification in this paper is based on the algebraic theory of stable fractional representations. This framework leads to an equivalent open-loop identification of a stable factorization of a nominal model and an allowable model perturbation written in terms of a (dual) Youla parameterization. Both the estimation of nominal factorization and the uncertainty estimation can be performed in a feedback relevant way, taking the intended control application of the estimated set of model into account.

The estimated set of models is used for the design of a robust controller for which significant improvement of the positioning mechanism has been illustrated.

ACKNOWLEDGMENT

The authors would like to thank Philips Research Laboratories, Eindhoven, The Netherlands, for providing the wafer stepper experimental setup. They would also like to thank O. Bosgra and D. de Roover for fruitful discussions and their contributions to this paper and E. Walgers for his contribution to the experiments.

REFERENCES

- [1] S. P. Boyd and C. H. Barrat, *Linear Controller Design—Limits of Performance*. Englewood Cliffs, NJ: Prentice-Hall, 1991.
- [2] R. A. de Callafon, D. de Roover, and P. M. J. Van den Hof, "Multivariable least squares frequency domain identification using polynomial matrix fraction descriptions," in *Proc. 35th IEEE Conf. Decision Contr.*, Kobe, Japan, 1996, pp. 2030–2035.
- [3] R. A. de Callafon and P. M. J. Van den Hof, "Control relevant identification for H_∞ -norm based performance specifications," in *Proc. 34th IEEE Conf. Decision Contr.*, New Orleans, LA, 1995, pp. 3498–3503.
- [4] —, "Filtering and parameterization issues in feedback relevant identification based on fractional model representations," in *Proc. 3rd European Contr. Conf.*, vol. 1, Rome, Italy, 1995, pp. 441–446.
- [5] —, "Suboptimal feedback control by a scheme of iterative identification and control design," *Math. Modeling Syst.*, vol. 3, pp. 77–101, 1997.
- [6] R. A. de Callafon, P. M. J. Van den Hof, and D. K. de Vries, "Identification and control of a compact disc mechanism using fractional representations," in *Proc. 10th IFAC Symp. Syst. Identification*, vol. 2, Copenhagen, Denmark, July 4–6, 1994, pp. 431–436.
- [7] R. A. de Callafon, "Feedback oriented identification for enhanced and robust control: A fractional approach applied to a wafer stage," Doctoral dissertation, Delft Univ. Technol., Delft, The Netherlands, 1998.
- [8] D. de Roover, "Motion control of a wafer stage: A design approach for speeding up IC production," Dr. dissertation, Delft Univ. Technol., Delft, The Netherlands, 1997.
- [9] J. C. Doyle, B. A. Francis, and A. R. Tannenbaum, *Feedback Control Theory*. New York: MacMillan, 1992.
- [10] G. C. Goodwin, M. Gevers, and B. Ninness, "Quantifying the error in estimated transfer functions with application to model order selection," *IEEE Trans. Automat. Contr.*, vol. 37, pp. 913–928, 1992.
- [11] R. G. Hakvoort and P. M. J. Van den Hof, "Identification of probabilistic uncertainty regions by explicit evaluation of bias and variance errors," *IEEE Trans. Automat. Contr.*, vol. 42, pp. 1516–1528, 1997.
- [12] A. J. Helmicki, C. A. Jacobson, and C. N. Nett, "Least squares methods for H_∞ control-oriented system identification," *IEEE Trans. Automat. Contr.*, vol. 38, pp. 819–826, 1993.
- [13] L. Ljung, *System Identification: Theory for the User*. Englewood Cliffs, NJ: Prentice-Hall, 1987.
- [14] —, *System Identification Toolbox User's Guide: The Mathworks, Inc.*, 1995.
- [15] P. M. Mäkilä and J. R. Partington, "On boundend-error identification of feedback systems," *Int. J. Adaptive Contr. Signal Processing*, vol. 9, no. 1, pp. 47–61, 1995.
- [16] P. M. Mäkilä, J. R. Partington, and T. K. Gustafson, "Worst-case control-relevant identification," *Automatica*, vol. 31, pp. 1799–1819, 1995.
- [17] B. Ninness and G. C. Goodwin, "Estimation of model quality," *Automatica*, vol. 31, pp. 1771–1797, 1995.
- [18] J. R. Partington and P. M. Mäkilä, "Analysis of linear methods for robust identification in l_1 ," *Automatica*, vol. 31, pp. 755–758, 1995.
- [19] R. J. P. Schrama, "Accurate identification for control design: the necessity of an iterative scheme," *IEEE Trans. Automat. Contr.*, vol. 37, pp. 991–994, 1992.
- [20] —, "Approximate Identification and Control Design with Application to a Mechanical System," Ph.D. dissertation, Delft Univ. Technol., Delft, The Netherlands, 1992.
- [21] R. J. P. Schrama and O. H. Bosgra, "Adaptive performance enhancement by iterative identification and control design," *Int. J. Adaptive Contr. Signal Processing*, vol. 7, no. 5, pp. 475–487, 1993.
- [22] T. Söderström and P. Stoica, *System Identification*. Englewood Cliffs, NJ: Prentice-Hall, 1989.
- [23] P. M. J. Van den Hof and R. J. P. Schrama, "Identification and control—Closed-loop issues," *Automatica*, vol. 31, no. 12, pp. 1751–1770, 1995.
- [24] P. M. J. Van den Hof, R. J. P. Schrama, R. A. de Callafon, and O. H. Bosgra, "Identification of normalized coprime plant factors from closed-loop experimental data," *European J. Contr.*, vol. 1, no. 1, pp. 62–74, 1995.
- [25] M. Vidyasagar, *Control System Synthesis: A Factorization Approach*. Cambridge, MA: MIT Press, 1985.
- [26] P. M. R. Wortelboer, "Frequency weighted balanced reduction of closed-loop mechanical servo-systems: Theory and tools," Ph.D. dissertation, Delft Univ. Technol., Delft, The Netherlands, 1993.
- [27] Z. Zang, R. R. Bitmead, and M. R. Gevers, "Iterative weighted least-squares identification and weighted LQG control design," *Automatica*, vol. 31, pp. 1577–1594, 1995.
- [28] K. Zhou, J. C. Doyle, and K. Glover, *Robust and Optimal Control*. Englewood Cliffs, NJ: Prentice-Hall, 1996.